International Journal of Computer Science Engineering
and Information Technology Research (IJCSEITR)
ISSN(P): 2249-6831; ISSN(E): 2249-7943
Special Edition, Apr 2015, 47-60

MICROANEURYSM DETECTION METHODS FOR DIABETIC RETINOPATHY

P MANOHAR[1], VIPULA SINGH[2] & KRISHNA R MURTHY[3]

[1]Department of Electronics and Instrumentation, R N S Institute of Technology, Bangalore, Karnataka, India

[2]Department of Electronics and Communication, R N S Institute of Technology, Bangalore, Karnataka, India

[3]Department of Vitreo Retina, Vittala International Institute of Opthalmology, Bangalore, Karnataka, India

ABSTRACT

Diabetic Retinopathy is an end-stage complication of Diabetes where the retina is damaged as a result of fluids leaking out of blood vessels into the retina. Image processing, analysis and computer vision techniques are employed to detect different lesions associated with Retinopathy. The presence of microaneurysms in the retina is the earliest sign of diabetic retinopathy. Early automated microaneurysm detection can help detect the onset of Diabetic Retinopathy. The number of microaneurysms is used to indicate the severity of the disease. In this paper, we review, classify and compare the algorithms and techniques used for the detection of microaneurysms from Diabetic Retinopathy retinal images.

KEYWORDS: Diabetes, Diabetic Retinopathy, Red Lesion, Microaneurysm, Retinal Image, Image Processing

I. INTRODUCTION

Diabetic Retinopathy (DR) is a chronic progressive, potentially sight threatening, retinal complication associated with diabetes [1]. The prevalence of DR is rising as a consequence of the epidemic of diabetes. It is predicted that by 2030 diabetes may afflict up to 79.4 million individuals in India [2]. A recent pooled analysis from 35 population based studies estimated that the number of people with DR will grow to 191.0 million by 2030 [3].

A healthy retina consists of blood vessels, optic disc and macula as its main components. DR is a progressive disease and its severity is determined by the number and the types of retinal lesions. DR is classified according to the presence or absence of abnormal new blood vessels as Non-Proliferative Diabetic Retinopathy (NPDR) and Proliferative Diabetic Retinopathy (PDR). NPDR comprises the early stages of the disease and is characterized by structural damage to small retinal blood vessels causing them to dilate and leak fluids. Microaneurysm (MA) is a vascular out pouching saccular enlargement of the retinal capillary. In digital photographs, the MAs appear as small, round shaped, red dots with less than 125 µm of diameter and with sharp margins. MAs may open and leak blood into the retinal tissue surrounding it thus forming hemmorhages which appear as red spots with irregular margins in digital retinal images. MAs and hemmorhages are red lesions while exudates and cotton wool spots are bright lesions. The chief component of exudates is proteins and lipids that have leaked from the blood stream into the retina through damaged blood vessels. Exudates exhibit as yellow regions with varying sizes and shapes. Cotton wool spots are white fluffy patches caused by arteriolar occlusion in that area of the retinal image. Depending upon the presence and extent of lesions, NPDR is classified into mild, moderate and severe. PDR is the advanced stage of DR. In this stage, the retina is deprived of oxygen and this triggers the growth of new blood vessels. These newly grown vessels are fragile and eventually leak blood leading to severe vision loss.

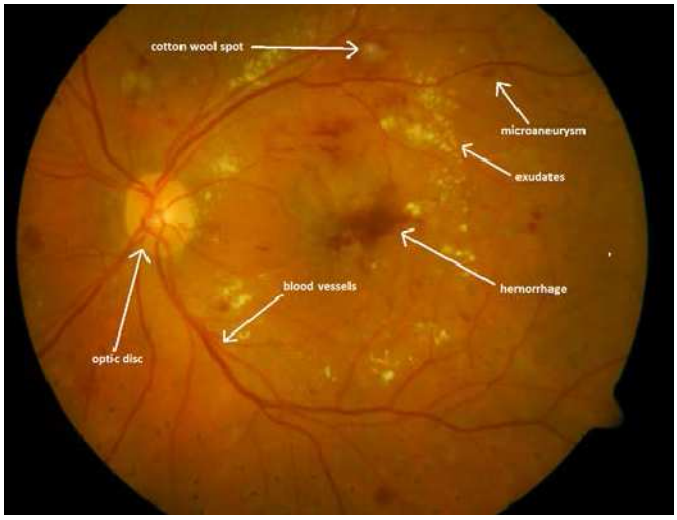

Figure 1: An Example of a Fundus Image Showing Different Types of Lesions [21]

The severity of DR generally parallels the duration of diabetes in diabetic patients [4]. Therefore, an effective treatment for DR requires early diagnosis and continuous monitoring of diabetic patients. Manual inspection of patient's retina for DR is rather slow, too laborious, and resource demanding. The delay between the patient being imaged and result of the reading can be days. Eye care experts in India are insufficient to support the growing diabetic population. A system that automatically detects DR can be a helpful auxiliary tool for the experts. This kind of automated system can provide faster detection and reduce the costs associated with the eye exams, thus improving the productivity and efficiency of the experts. Other benefits include improved repeatability and immunity from fatigue. Furthermore, the automated system can be used for grading the images based on the severity levels of DR. DR screening conducted over a larger population can become efficient if the automated system can separate normal and abnormal cases, instead of the manual examination of large voluminous image data.

MAs are the first clinically observable lesions indicating DR. Therefore MAs play a very important role in the early detection of DR. The objective of this paper is to review the relevant literature in the field of MA detection, and to provide researchers with a detailed resource of MA detection algorithms.

The paper is organized as follows. Section I gives an introduction to DR and automatic detection of DR. Section II describes the general process of automated MA detection. In Section III several different preprocessing methods of digital retinal images have been discussed. Different methods for the segmentation and removal of optic disc and blood vessels are included in this section. Section IV presents the methods for detection of microaneurysms. Section V discusses the comparison results of described methods discussed in section IV. Finally section V contains the conclusion.

II. AUTOMATED MA DETECTION SYSTEM

Figure 2 shows the general process of automated MA detection. Digital retinal images are processed in an algorithm sequence with output of one stage forming input to the next.

Fundus photography is the creation of a digital photograph of the interior layers of the eye, including the retina, optic disc, macula and posterior pole. For large scale screening, fundus cameras are more reliable for acquiring the fundus images.

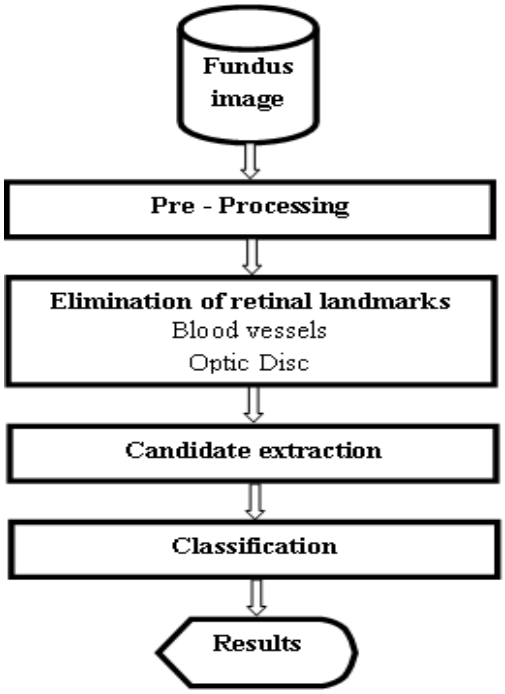

Figure 2: The general Process of Automated MA Detection

PREPROCESSING AND ELIMINATION OF RETINAL LANDMARKS

A. Preprocessing

The input image from the fundus image database is preprocessed to enhance the contrast of the image, to correct for image non-uniformity, to normalize colour, and to reduce noise.

The varying contrast and non-uniform shade across the retinal images can make the detection of MAs a challenging task as feature extraction algorithms work accurately on images with good contrast and no background variations. Dark lesions like MAs are very similar to the background in fundus images. Therefore preprocessing for contrast enhancement is essential to intensify the contrast between the areas of interest and the background. Many fundus images suffer from non-uniform illumination since the incident light has to be flashed in through the pupil as the image is acquired and the spherical geometry of the eye creates significant inter reflection and shading artefact [5].

Colour normalization is necessary to reduce the intra image and inter image variability in the colour of the retina in different patients. Sometimes the presence of noise in a fundus image can be confused for a true MA. Filtering is necessary to reduce the image noise.

Retinal images typically have a limited field of view (FOV) mainly due to the curvedness of the retina. To maximize the FOV of retinal image, it is first resized while maintaining the same aspect ratio and then its redundant lines and rows are trimmed.

Retinal images are always saturated in the red channel and have very low contrast in the blue channel. Green plane of the colour fundus image is considered in many related papers since the contrast between MAs and retinal area is the highest in green plane. In inverted green channel fundus image, MAs, hemmorhages and the vasculature will appear as bright structures.

Jorge Oliveira et al. [6] used the green channel image. The image was resized to a width of 768 pixels and its

redundant lines and rows were trimmed using a mask to maximize the field of view (FOV). A shade correction was applied to the inverted green plane image to remove the variability in lighting and slow varying structures. The shade corrected image was normalized which allowed comparing the intensities among regions from the same image. A threshold value of 0.68 was used to binarize the normalized image.

Tsuyoshi Inoue et al. [7] and Atsushi Mizutani et al. [18] used brightness correction, gamma correction and contrast enhancement techniques for reducing the differences in brightness and contrast in the unprocessed retinal images. For reducing the noise, a low pass filter based on Fast Fourier Transform was applied to the green channel component of the colour image.

M. UsmanAkram [8] used morphological opening for smoothing of bright lesions and optic disc. Contrast enhancement technique was applied to the green plane of the image in order to enhance the contrast of lesions for easy detection. Gabor filter banks were then used for further enhancement of regions with possible MAs. The candidate regions for MAs and Hemmorhages were extracted from Gabor filter output by applying a low threshold value.

Istvan Lazar et al. [9] used the inverted green channel of the fundus image because MAs, Hemmorhages and the vascular tree appear as bright structures in an inverted image. Input images with an ROI (region of interest) of 540 pixels were considered. To suppress noise and to preserve true MAs, image smoothing was performed on the input image using convolution with a Gaussian mask of variance 1. MAs are local intensity maximum structures. Local maximum regions (LMRs) of the preprocessed image were considered as the possible MA candidate regions. This reduced the number of pixels to be processed.

Marwan D. Saleh et al. [10] used green channel extraction because green channel provides maximum local contrast among the image pixel values. Morphological top and bottom hat transforms were used to perform the contrast enhancement. Image background was removed by subtracting the contrast enhanced image from the median filtered image. Contrast stretching was then performed on the difference image to cover the full dynamic range.

Victor Murray et al. [11] used intensity normalization for all the images so that they have the same mean intensity values.

L. Giancardo et al. [12] used the green channel image and resized it using bilinear interpolation. In order to maximize the FOV, the image was cropped based on the redundant rows and columns of the mask. The background is estimated by a median filter applied to the inverted green channel image. The background image is then subtracted from the inverted green channel image and is normalized with $\mu = 0.5$ and $\sigma = 0.2$. From the normalized image, pixel values with different pigmentation, contrast and illumination can be compared. The normalized image was divided into 5×5 valid windows where each valid window contained at least one candidate pixel. Each valid window was centred on the pixel with maximum intensity in its 5×5 neighbourhood. With this, the probability of the suspected MA in the middle of the window is higher.

Keerthi Ram et al. [14] performed preprocessing on the green colour plane of the colour fundus image in order to minimize the effect of intensity variation in the image background. To normalize the background, an estimate of the background obtained by median filtering was subtracted from the green plane image. Dark and small size MAs with a low intensity value in a normalized image were then enhanced by morphological bottom hat enhancement.

Akara Sopharak et al. [15] used a median filtering operation on the green plane image to attenuate the noise.

Contrast limited adaptive histogram equalization was applied to highlight the lesion visibility. To remove background variation due to non-uniform illumination, a shade correction algorithm was applied to the green plane image.

Abhir Bhalerao et al. [19] applied median filter to remove salt and pepper noise. For eliminating regions with low contrast, the median filtered output was multiplied by a local mean filtered image. A contrast normalized image was obtained from the shading bias.

B. Elimination of Retinal Landmarks

MAs cannot occur on vessels but they appear as disconnected from the vessels. Smaller hemorrhages and MAs are often similar in color, geometry and texture to the thin blood vessels. The crossings of thin blood vessels may result in round spots similar to MAs both in size and shape. Hence, blood vessel pixels need to be removed prior MA detection for reducing the number of false positives. The fovea is mostly detected as a red lesion since it appears with similar features as red lesions. Some dark small spots could appear inside the optic disc which may be incorrectly detected as MAs. Hence, optic disc removal helps to remove those confusing dark spots.

Tsuyoshi Inoue et al. [7] used a combination of double ring filter and black hat transform to delete the blood vessels from the candidate regions of MA.

M. UsmanAkram et al. [8] used 2D Gabor wavelet on the inverted green channel for blood vessel enhancement especially the thin and less visible vessels. Multilayered thresholding and adaptive thresholding techniques were applied to create a binary mask for blood vessel segmentation. Blood vessels were then marked by assigning one to all those pixels which belonged to blood vessels and zero to non vessel pixels.

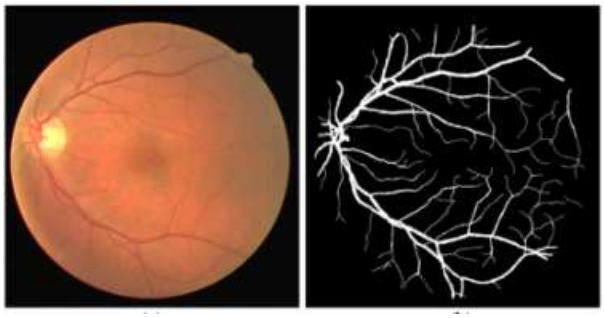

(a) **(b)**

Figure 3: (a) Original Image b) Blood Vessels Detected [26]

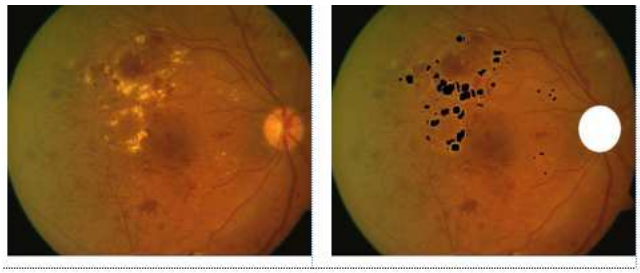

Figure 4: (a) Original Image (b) Image with Exudates in Black Colour and Optic Disc Masked out [17]

Akara Sopharak et al. [15] obtained the vessel candidate areas by taking the difference of two images. The first

image was generated by using a closing operator that eliminated the vessels from the preprocessed image. A flat disc shaped structuring element of radius 10 was used. A second image was obtained by using a filling operation that removed small red objects with diameters less than the size of MA. The candidate vessels were then binarized by thresholding.

Saiprasad Ravishankar et al. [17] performed closing operations on the green channel image using two disk shaped structuring elements of different sizes S1 and S2. With this vessels which are the thin dark segments were closed. S2 was fixed at a high value of 6 pixels and S1 was fixed at 4 pixels less than S2. The difference image containing the entire blood vessel network was obtained by taking the difference of the two closed images. The difference image was then thresholded and median filtered to obtain the binary image of the blood vessels. Morphological thinning was then performed on the binary image to obtain the skeleton of the blood vessel network.

Optic disc is an important retinal feature and can be used to diagnose other retinal diseases like Glaucoma. Marwan D. Saleh et al. [10] used median filtering to fill up the thin blood vessel region inside optic disc. The contrast of the resulting image was then enhanced based on morphological top hat transform. The low contrasted image obtained from top hat operation was then contrast stretched in order to cover the full dynamic range of the image. The resulting image was converted to a binary image. Morphological opening and closing operations were utilized to detect the rough location of the optic disc. To detect the accurate location of the optic disc and also to discriminate the optic disc from bright lesions a method based on Centroid Distance Method was used.

Saiprasad Ravishankar et al. [17] proposed a new method of optic disc detection where they first detected the major blood vessels and used the intersection of those to find the approximate location of the optic disc. The optic disc was detected by combining the major blood vessel convergence and high intensity property of disk regions in a cost function.

Atsushi Mizutani et al. [18] eliminated the pixels corresponding to blood vessels using a double ring filter with inner and outer diameters of 7 and 21 pixels respectively.

METHODS USED FOR MA DETECTION

Although shown separately in Figure 2, MA candidate extraction and classification are overlapping by nature. Candidate extraction is a process that aims to spot any objects in the preprocessed image showing MA like characteristics by excluding regions which do not have similar characteristics to MAs. The extracted candidates are subjected to classification to eliminate false positives.

Jorge Oliveira et al. [6] presented Slant stacking, a formulation of the Radon transform, to automatically detect MAs. The Radon transform of a MA is a linear structure. An interesting characteristic of this formulation is that the shape in the Radon domain is invariant to the position of the MA in the window. The Radon transform was applied to an MA candidate and a set of 21 features from the Radon domain was extracted. Iterative segmentation of the slant stacking image involved binarization with the highest threshold, so that a connected object connecting both extremities of the transform domain is produced. This enabled the extraction of more convenient features. Features based on intensity, threshold level, complexity and slope and offset, mean and variation were extracted and normalized. Principal Component Analysis (PCA) was used to reduce the number of features. SVM classifier with RBF kernel was used. A 5 fold cross validation method was used to train the classifier. A grid search method was used to obtain the hyperparameters for each iteration. The final result was the mean of all iterations.

Tsuyoshi Inoue et al. [7] proposed detection of MA candidate regions by using Eigen values based on a Hessian matrix. The Eigen values of the Hessian matrix were used to classify the shape of the intensity curve surface. When shape index has a small value, the possibility of MA is high. The detected candidate region was different from its actual size. Hence candidates were modified in the regions by re-thresholding the eigen value in the Hessian matrix. 126 features based on pixel value, shape and texture analysis were calculated for each candidate region. 126 features were reduced to 25 components by Principal Component Analysis (PCA) and then fed to ANN classifier. False positive candidates were removed by a threshold operation based on feature analysis. ANN classifier using back propagation method was used to classify the candidate regions as MA or false positive.

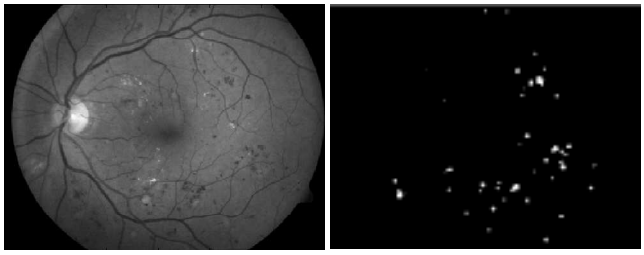

(a) **(b)**

Figure 5 a) Original Image b) MAs Detected [22]

M. UsmanAkram et al. [8] used Gabor filter to extract the candidate regions of MAs and hemmorhages. A feature vector for each candidate region was formed using the properties like color, area and shape of the region, gray level intensities inside the region and statisitical properties like entropy, energy and moments. Supervised Local Fisher Discriminant Analysis (LFDA) was used to further enhance the feature space formed for each candidate region. A hybrid classifier which is a weighted combination of three classifiers namely Gaussian Mixture Model (GMM), Support Vector Machine (SVM) and Multimodel mediod (M-mediod) was used to separate MA and non MA regions. Hybrid classifier gave better accuracies as compared to individual classifiers.

Istvan Lazar et al. [9] proposed MA detection based on the principle of analysing directional cross section profiles centred on the local maximum pixels of the preprocessed image. A set of cross section intensity profiles were obtained by recording the intensity values along discrete line segments of different orientations of the central candidate pixel. On the obtained cross section profiles, peak detection was performed and several attributes regarding the shape, size and height of the peak were calculated. The final feature set consisting of a set of statistical measures was formed that showed how the attributes of the peak vary with the orientation of the cross section changes. Naive Baye's classifier was used to exclude the spurious candidates. Score values to the MA candidates that were classified as true MAs were assigned. More visible MAs achieved higher score than faint ones. Nonmaximum suppression was then performed which is an operation of selecting a point with the highest score from every maximum region.

Marwan D. Saleh et al. [10] used h – maxima transformation and multi level thresholding for segmenting dark spot lesions namely MAs and HAs. h – maxima transformation reduced the number of intensity levels by suppressing the maxima in the image whose values were less than a certain threshold. Features like object density and the ratio of major to minor axes were calculated for each of the labelled objects in the binary image. With suitable threshold values false positives such as blood vessels and other unwanted objects were then removed. Geometric based criteria were used to classify MAs and HAs. Features such as size, shape, major and minor axes of each object, ratio of an object area to a

convex area were used for classification. Based on the number and location of MAs and HAs, the severity level was graded into normal, mild, moderate and severe.

L. Giancardo et al. [12] proposed a new MA segmentation technique based on a novel Radon based approach. The Radon Transform was applied to the normalized image to obtain the Radon space. The Radon space was analysed to separate the MAs from other dark structures such as vessels and noise. A vector containing the mean across the rows of window will have a strong maximum in the middle even if another dark structure like vessel is present at the periphery of the window along with MA. The Standard deviation across the rows of the window is employed to discriminate between MAs and vessel bifurcations. Principal Component Analysis (PCA) and SVM classifier were used to classify the new set of features obtained from the Radon space analysis. The original feature vector having 37 dimensions was projected to a hyperplane of 10 dimensions through Principal Component Analysis. Features obtained through PCA were then classified with SVM classifier. The SVM classifier obtained a score of 0.96 AUC after PCA dimensionality reduction. Finally a score representing the likelihood of containing a MA to each window was assigned.

Li Tang et al. [13] proposed an algorithm for hemmorhage detection based on splat feature classification. The entire fundus image was partitioned into a number of non overlapping splats. A set of distinct features were extracted from each splat. Hemmorhages share the same appearance features with the vasculature. So, the splat based classifier was trained with a set of features extracted from blood vessels. The vasculature and the haemorrhages were separated from the rest of the retina by the classifier.

Keerthi Ram et al. [14] considered two classes which were true MAs (Pc) and non MAs (PT) in a given image. The probability that a candidate belongs to a true MA is small compared to that of non-MA class. MA detection problem was formulated as a problem of target detection embedded in a background clutter, where the target occurs with much lower probability compared to the clutter. A two stage cascade of rejectors was used to reduce Pc while maintaining PT. Culling of clutter by two stages passed the majority of true MAs. Finally, the true positives that remained after the final rejector were assigned a similarity score [0 – 1] based on their similarity to true MAs.

Akara Sopharak et al. [15] proposed a method for MA detection from non dilated pupil digital fundus images. A set of optimally adjusted morphological operators were used for MA detection. The method detected MA by its diameter and connected pixels. The h-transform was applied to the preprocessed image to suppress all the minima of depth less than or equal to a predefined threshold. The h-minima transform is a thresholding technique which produced a binary image where the white pixels represented the regional minima in the original image. Regional minima are connected pixels with the constant intensity value whose external boundary pixels all have a higher value. The threshold value was calculated using Otsu algorithm.

Luca Giancardo et al. [16] presented a technique for the detection of MA using Radon Transform for detecting single circular Gaussian like structures regardless of their size and strength. The circular Gaussian structures appear as a continuous chain of cliffs when observed in the Radon space. Three properties namely location in the window, size and intensity of the circular Gaussian shape were studied from the Radon cliffs. The location of the Gaussian shape in the window was deduced from the shape of the crest, the size from the width of the cliffs and the intensity from the height of the cliffs. Two measures, path votes (p_{votes}) and cumulative peak probability (CPP) were obtained by using a sliding window centred on each candidate pixel. The candidate was considered for further processing for $p_{votes} > 4$ and then the probability of being a MA was calculated.

Saiprasad Ravishankar et al. [17] proposed a method to automatically detect MAs in fundus images using morphological operations. Morphological filling was performed on the green channel image. The unfilled green channel image was then subtracted from the filled one and thresholded to get an image with MA patches. The blood vessel network was first obtained. It was dilated and subtracted from the thresholded image to remove the noise due to blood vessels. The fovea was removed since it appears commonly in MA and hemmorhage detection. The fovea was detected using the location of the optic disc and curvature of the main blood vessel. The size, count and distribution of MAs were used to predict the severity of Diabetic Retinopathy.

Atsushi Mizutani et al. [18] proposed a method for detecting MA candidate regions by using a double ring filter. Double ring filter with inner and outer rings of 5 and 13 pixels respectively was used. MAs appear darker than the surrounding retinal regions and double ring filter compares the target pixel values with the neighbouring pixel values. If average pixel in the inner circle was found lower than the neighbouring pixels in the outer ring region then the pixel under consideration was a candidate MA pixel. To remove the false positives, 12 features were calculated for each candidate lesion. Rule based classifier and ANN classifier used these features for classifying MAs and false positives.

Abhir Bhalerao et al. [19] presented a model based approach that employed standard linear filtering and eigen image value analysis. The orientation matched filter is applied on the preprocessed image and the output of the filter is thresholded to get a set of potential candidates. Intensity and shape filters using a circular symmetric operator are employed on an orientation map of the input. An eigen image morphological analysis of the candidate regions is done to reduce the false positive rate.

Gary G. Yen et al. [20] proposed a hybrid intelligent system (HIS) with multilevel knowledge representation to construct a DR sorting system based on ETDRS protocol. The proposed system sorted the images according to their severity level. The regions of interest of a given fundus image were segmented and the features of interest were automatically extracted. Among the features extracted, feature sets were grouped according to the ETDRS protocol and fed to HIS. The specific region of fundus image was categorized into MAs, hemmorhages, hard exudates, soft exudates and drusen.

V.EVALUATION AND PERFORMANCE MEASURES

Researchers came up with many measures to evaluate the performance of their algorithms. The performance evaluation is made either at pixel level, lesion level or image level. In pixel based evaluation, pixel by pixel evaluation is done by comparing the detected MAs with ground truth image pixels. In lesion based evaluation, number of MAs is used for comparison. Image based evaluation is widely used in which correct classification of images into normal or abnormal images is used to evaluate the detection algorithm. The most commonly used performance measures are Sensitivity and Specificity. Sensitivity is a measure of proportion of positives which are correctly detected. Specificity is a measure of proportion of negatives which are correctly detected. The value of Sensitivity and Specificity lies between 0 and 1. Accuracy is a measure of total proportion of positives and negatives which are correctly detected. There is some work in the literature where the average number of false positives per image (fppi) is used as one of the performance evaluation values.

$$Sensitivity = \frac{TP}{TP + FN} \quad (1)$$

$$Specificity = \frac{TN}{TN + FP} \tag{2}$$

$$Accuracy = \frac{TP + TN}{TP + FP + FN + TN} \tag{3}$$

where in a pixel based evaluation

True Positive (TP) is the number of MA pixels correctly detected,

False Positive (FP) is the number of non-MA pixels which are wrongly detected as MAs,

False Negative (FN) is the number of MA pixels that are not detected,

True Negative (TN) is the number of non-MA pixels which are correctly identified as non-MA pixels.

The value of Sensitivity and Specificity should be high for better MA detection results. Many researchers have been working on improving algorithms for detection of DR with sufficient Sensitivity. Sensitivity is more important than Specificity because the case of sight threatening retinopathy should not be missed out. Sensitivity is a safety issue while Specificity is an efficiency issue. The effectiveness of each stage of the automated MA detection process must be high to ensure that the effectiveness of the overall process is maintained at a satisfactory level of Sensitivity and Specificity.

The performance of MA detection results is analysed with ground truth images available in the corresponding datasets. Algorithms are evaluated on publically available validated digital image libraries like DRIVE [23], STARE [24] and DIARETB1 [25]. DRIVE (Digital Retinal Images for vessel extraction) database consists of 40 colour fundus images where each image was captured using 8 bits per color plane at 768×584 pixels. STARE (STructured Analysis of the Retina) database consists of 396 colour fundus images, where each slide was digitized to produce a 605×700 pixel image, 24 bits per pixel. DIARETB0 and DIARETB1 (Standard Diabetic Retinopathy) databases consists of 130 and 89 images respectively with a size of 1500×1152 pixels. Images in each datasets are divided into training and testing sets. Other important datasets are MESSIDOR, REVIEW, HEI-MED, ROC_d and DRiDB.

Table 1 shows the results of MA detection methodologies reviewed in section IV. The methods described in this paper are not compared on the same database thus making direct comparisons between methods very difficult.

Table 1: Performance of Algorithms

Authors	Performance Measures	
	Sensitivity	Specificity
Jorge Oliveira [6]	89.46%	84.16%
M. UsmanAkram [8]	98.64%	99.69%
Marwan D. Saleh [10]	84.31%	93.63%
Victor Murray [11]	89%	59%
Akara Sopharak [15]	81.61%	99.99%
Saiprasad Ravishankar [17]	95.1%	90.5%
Abhir Bhalerao [19]	82.6%	80.2%
Tsuyoshi Inoue [7]	Sensitivity of 0.73 at 8 fppi.	
Istvan Lazar [9]	Sensitivity of 0.251 at 1/8 fppi.	
L. Giancardo [12]	Sensitivity of 0.366 at 0.5 fppi.	
Keerthi Ram [14]	Sensitivity of 0.8846 at 18 fppi.	
Luca Giancardo [16]	Sensitivity of 0.25 at 1 fppi	
Atsushi Mizutani [18]	Sensitivity of 0.65 at 27 fppi.	
Gary G. Yen [20]	Sensitivity of 0.9355 with eight images wrongly sorted.	

Usman Akram et al. [8] could obtain a high Sensitivity and Specificity because the proposed system focussed on improving the accuracy of each stage in order to have an overall higher accuracy. Jorge Oliveira et al. [6] obtained slightly low Specificity because the candidate extractor detected more number of non-MAs than MAs. Victor Murray et al. [11] explains that the Sensitivity can be increased if better preprocessing methods are used to reduce noise or small image artifacts that mimic small lesions like MAs.

CONCLUSIONS

The early signs of DR can be notified by the presence of MAs in fundus images and hence the need for effective MA detection algorithms is inevitable. Evaluation of an automatic DR detection system using existing algorithms cannot yet be recommended for clinical practice because the false negative rate is still not acceptable and the processing time is still slow. Therefore, there is a compelling need for improvement in the performance of detection algorithms. This work gives the depiction of the various stages involved in the diagnosis of DR and reviews existing MA detection methods. It can act as a resource for the future researchers interested in automated MA detection and help them to get a complete view of this field.

REFERENCES

1. Scientific Department, The Royal College of Ophthalmologists, Diabetic Retinopathy Guidelines December 2012, July 2013.
2. Wild S, Roglic G, Green A, Sicree R and King H, " Global Prevalence of Diabetes: Estimates for the year 2000 and projections for 2030", Diabetes Care. 27(5):1047-53. May 2004.
3. Yingfeng Zheng, Mingguang He, and Nathan Congdon, "The Worldwide Epidemic of Diabetic Retinopathy", Indian J Ophthalmol. 60(5): 428–431, Sep-Oct 2012.
4. Comprehensive Ophthalmology by A.K. Khurana, 4rth edition. New Age International limited publishers.
5. Abhir Bhalerao, Sarabjot Anand and Ponnusamy Saravanan "Retinal Fundus Image Constrast Normalization using Mixture of Gaussians", 42nd Asilomar Conference on Signals, Systems and Computers, Pacific Grove, CA, Oct 2008.
6. Jorge Oliveira, Graca Minas and Carlos Silva, "Automatic Detection of Microaneurysm Based on the Slant Stacking", IEEE 26th International Symposium on Computer-Based Medical Systems (CBMS), June 2013, pp.308-313.
7. Tsuyoshi Inoue, Yuji Hatanaka, Susumu Okumura, Chisako Muramatsu, and Hiroshi Fujita, "Automated Microaneurysm Detection Method Based onEigenvalue Analysis Using Hessian Matrix in Retinal Fundus Images",IEEE 35th Annual International Conference, Engineering in Medicine and Biology Society (EMBC), July 2013, pp. 5873-5876.
8. M. UsmanAkram, ShehzadKhalid and ShoabA.Khan "Identification and classification of microaneurysms for early detection of diabetic retinopathy", Elsevier, Pattern Recognition 46, 2013, pp.107-116.
9. Istvan Lazar and Andras Hajdu, "Retinal Microaneurysm Detection Through Local Rotating Cross-Section Profile Analysis", Medical Imaging, IEEE Transactions Volume:32 , Issue: 2, Nov 2012, pp. 400 – 407.

10. Marwan D. Saleh and C. Eswaran, "An automated decision-support system for non-proliferative diabetic retinopathy disease based on MAs and HAs detection" Elsevier, Computer methods and programs in biomedicine, 2012, pp. 186-196.

11. Victor Murray, Carla Agurto, Simon Barriga, Marios S. Pattichis, and Peter Soliz, "Real time Diabetic Retinopathy patientscreening using multiscale AM-FM methods", 19th IEEE International Conference, Image Processing (ICIP), Oct 2012, pp.525-528.

12. L. Giancardo, F. Meriaudeau, T. P. Karnowski, "Microaneurysm Detection with Radon Transform-based Classification on Retina Images", IEEE Annual International Conference on Engineering, Medicine and Biology Society, EMBC, Aug – Sep 2011, pp. 5939 – 5942.

13. Li Tang, Meindert Niemeijer and Michael D. Abramoff, "Splat Feature Classification Detection of the presence of large retinal Hemmorhages", IEEE International Symposium, Biomedical Imaging: From Nano to Macro, Mar-Apr 2011, pp.681 - 684.

14. Keerthi Ram, Gopal Datt Joshi and Jayanthi Sivaswamy, "A Successive Clutter-Rejection-Based Approach for Early Detection of Diabetic Retinopathy" IEEE Transactions on Biomedical Engineering, VOL. 58, No. 3, Mar 2011, pp 664-673.

15. Akara Sopharak, Bunyarit Uyyanonvara and Sarah Barman, "Automatic Microaneurysm Detection from Non-dilated Diabetic Retinopathy Retinal Images Using Mathematical Morphology Methods", IAENG International Journal of Computer Science, 38:3,IJCS_38_3_15, Aug 2011.

16. Luca Giancardo, Fabrice Meriaudeau, Thomas P. Karnowski, Kenneth W. Tobin*a*, Yaqin Li*c* and Edward Chaum, M.D. "Microaneurysms Detection with the Radon Cliff Operator in Retinal Fundus Images", Medical Imaging: Image Processing, Proc. of SPIE Vol. 7623 76230U-1, 2010.

17. Saiprasad Ravishankar, Arpit Jain and Anurag Mittal "Automated Feature Extraction for Early Detection of Diabetic Retinopathy in Fundus Images", IEEE Conference, Computer Vision and Pattern Recognition CVPR, Jun 2009, pp. 210-217.

18. Atsushi Mizutani, Chisako Muramatsua, Yuji Hatanaka, Shinsuke Suemoria, Takeshi Haraa and Hiroshi Fujitaa, "Automated microaneurysm detection method based on double-ring filter in retinal fundus images", Medical Imaging: Computer-Aided Diagnosis, Proc. of SPIE Vol. 7260 72601N-1, 2009.

19. Abhir Bhalerao, Amiya Patanaik, Sarabjot Anand and Pounnusamy Saravanan, "Robust Detection of Microaneurysms for Sight Threatening Retinopathy Screening", Sixth International Conference, Computer Vision, Graphics & Image Processing ICVGIP. 2008.

20. Gary G. Yen and Wen-Fung Leong, "A Sorting System for Hierarchical Grading of Diabetic Fundus Images: A Preliminary Study", IEEE Transactions on Information Technology in Biomedicine, Vol. 12, No. 1, Jan 2008.

21. Smith Gulati, Nutnaree Kleawsirikul, and Bunyarit Uyyanonvara, "A Review on Hemorrhage Detection Methods for Diabetic Retinopathy Using Fundus Images", International Journal of Biological, Ecological and Environmental Sciences (IJBEES) Vol.1, No.6, 2012

22. Hussain F. Jaafar, Asoke K. Nandi and Waleed Al-Nuaimy, “Automated Detection of Red Lesions from Digital Colour Fundus Photographs ”, 33rd Annual International Conference of the IEEE EMBS, Aug-Sep 2011
23. J. J. Staal, M. D. Abramoff, M. Niemeijer, M. A. Viergever, and B. van Ginneken, Digital Retinal Image for Vessel Extraction (DRIVE) Database, Image Sciences Institute, University Medical Center Utrecht, 2004, http://www.isi.uu.nl/Research/Databases/DRIVE/.
24. M. D. M. Goldbaum, STARE Dataset Website, Clemson University, Clemson, SC, USA, 1975, http://www.ces.clemson.edu.
25. T. Kauppi, V. Kalesnykiene, J. K. Kamarainen, L. Lensu, I. Sorri, A. Raninen, R. Voutilainen, H. Uusitalo, H. K¨alvi¨ainen, and J. Pietil¨a, “DIARETDB1 diabetic retinopathy database and evaluation protocol,” presented at the Medical Image Understanding Analysis, 2007.
26. http://projects.i-ctm.eu/en/project/blood-vessel-segmentation